Journal of Fluorescence, Vol. 15, No. 5, September 2005 (© 2005)
DOI: 10.1007/s10895-005-2990-8

Polar Plot Representation for Frequency-Domain Analysis of Fluorescence Lifetimes

Glen I. Redford[1] and Robert M. Clegg[1,2]

Received May 3, 2005; accepted July 19, 2005

We present applications of polar plots for analyzing fluorescence lifetime data acquired in the frequency domain. This graphical, analytical method is especially useful for rapid FLIM measurements. The usual method for sorting out and determining the underlying lifetime components from a complex fluorescence signal is to carry out the measurement at multiple frequencies. When it is not possible to measure at more than one frequency, such as rapid lifetime imaging, specific features of the polar plot analysis yield valuable information, and provide a diagnostic visualization of the participating fluorescent species underlying a complex lifetime distributions. Data are presented where this polar plot presentation is useful to derive valuable, unique information about the underlying component distributions. We also discuss artifacts of photolysis and how this method can also be applied to samples where each fluorescence species shows a continuous distribution of lifetimes. Polar plots of frequency-domain data are commonly used for analysis of dielectric relaxation experiments (Cole–Cole plots), which have proved to be exceptionally useful in that field for decades. We compare this analytical tool that is well developed and extensively used in dielectric relaxation and chemical kinetics to fluorescence measurements.

KEY WORDS: Fluorescence lifetimes; frequency-domain; FLIM; polar plot.

INTRODUCTION

The lifetime of a fluorescence signal provides valuable information about the environment of a fluorophore on the molecular scale, and this is especially valuable for biological studies. The techniques for fluorescence lifetime acquisition and analysis are usually subdivided into time-domain acquisition [1] and frequency-domain techniques [2–5]. The frequency domain is often preferred because the acquisition is relatively rapid, and the electronics are simpler. There are advantages to both time- and frequency-domain acquisition, but the basic time-dependent formalism is identical [6,7]. Fluorescence decay processes are often analyzed according to a minimum model of a single lifetime component; however, usually the system has multiple lifetime components or a more complex distribution of lifetimes. In this case, time-domain acquisition systems usually fit the signal as multi-exponential decays to determine separate lifetime components (or lifetime distributions). Frequency-domain methods typically perform measurements at multiple frequencies of excitation to determine the phase and modulation amplitudes at different frequencies. These data are then fit to models that are Fourier transforms of multi-exponential time-domain models. For fluorescence lifetime imaging with very rapid acquisition (approximately video rates [7]), where large amounts of data are acquired in a short time, frequency-domain instruments usually use only one frequency. This limits the ability to detect multiple lifetime components directly.

This paper discusses an analysis procedure that is applicable to single-frequency measurements of samples

[1] Physics Department, University of Illinois, Urbana-Champaign, Illinois.
[2] To whom correspondence should be addressed at Loomis Laboratory-Physics, 1110 West Green Street, Urbana-Champaign, Illinois. E-mail: rclegg@uiuc.edu

exhibiting more than one fluorescence lifetime. The analysis is also useful for globally analyzing multiple frequency components; however, in this paper we limit the discussion to a single frequency. It is a simple procedure to extend the polar plot analysis to each frequency component of a multi-frequency data set. We have been applying this method in the last few years to our FLIM data, and it has given us unique insights and has aided us in interpretation [8,9]. The methodology offers a simple, graphical, rapid algorithm for interpreting the phase and modulation data of a single-frequency measurement, which can be of great assistance in the interpretation of lifetime distributions. The analysis is particularly important in lifetime imaging where the low signal-to-noise makes standard analysis techniques impracticable, where large individual data sets are collected at every pixel of a CCD camera, and where signals are analyzed in terms of single frequencies.

The representation of fluorescence data presented in this paper is formally identical to well-known procedures used over many decades for the analysis of dielectric relaxation experiments (see Appendix C). It is applicable for analyzing signals derived from the dynamic behavior of any chemical or physical system relaxing due to repetitive time-dependent perturbations. In fluorescence, the perturbation is the excitation light, and the relaxation is the detected fluorescence emission. The analysis procedures and parameter transformation has been used extensively for analyzing transient responses to perturbations, such as dielectric dispersion [10–15] analysis of AC circuits [14], and chemical relaxation kinetic experiments [16]. Its use for fitting and displaying data from dielectric relaxing systems with two lifetimes in a polar plot has been demonstrated in the field of dielectric relaxation [11,17]. Recently, this graphical method has been applied to frequency-domain data from fluorescence lifetime images [18] for fitting signals from continuously variable ratios of two fluorescent species. The polar plot has been used as a graphic demonstration that the effective modulation lifetimes at any single frequency are longer than the phase lifetimes for frequency-domain fluorescence lifetime measurements of multi-component fluorescence [19].

In this paper, we discuss some details of the general theory behind this analysis and show how this method can be applied to analyze data from our real-time fluorescence lifetime imaging instrument. The graphical analysis is independent of any underlying physical model, and is associated directly with the experimental data. We also show how this method can be used for interpreting more complex data from component distributions rather than combinations of specific single components. And we discuss how artifacts, such as photo-bleaching, affect the analysis and the graphical display of the data.

THE TIME COURSE OF FLUORESCENCE DECAY

First we define the parameters. Those familiar with the usual representation of frequency-domain measurements might want to skip the next section.

The fundamental dynamic process of fluorescence is described in terms of the time-dependent fluorescence emission in response to very short pulses of excitation light (delta functions). Following such an excitation event, each species of excited fluorophore will decay as a single exponential. In general, multiple fluorescent species are present, and the time course of the fluorescence decay consists of a sum of exponential decay processes,

$$F(t) = \sum_i a_i e^{-t/\tau_i}, \tag{1}$$

where τ_i is the ith fluorescence lifetime and a_i is the amplitude of the ith component [3,20–23].

The basic measurement in the time domain involves a short pulse of light to excite the fluorophores into an excited state. The time course of the fluorescence signal is recorded directly as the excited molecules decay to the ground state. In order to achieve sufficient signal-to-noise, the signal is usually acquired and averaged over many pulses. Often the excitation light pulse is not negligibly short compared to the fluorescence relaxation times, and the measured fluorescence signal then becomes the convolution of the delta function response given in Eq. (1) with the form of the excitation pulse, $E(t')$,

$$F_{\text{meas}}(t) = \int_0^t E(t')F(t-t')\,dt'. \tag{2}$$

The exponential time constants and amplitudes are then determined by de-convolving the fluorescence response of Eq. (1) from the measured fluorescence signal, knowing the time dependence of $E(t')$. There are many ways to acquire data in the time domain, and we refer the reader to the literature for details [24–28]. Measuring the fluorescence decay directly in the time domain requires that the repetition period of the short light pulses be a good deal longer than the fluorescence lifetimes, in order to acquire the whole decay process and avoid pulse pile-up.

THE FREQUENCY-DOMAIN MEASUREMENT

Equation (2) is very general. Every measurement of fluorescence decay can be described by Eq. (2), even though the excitation event may not be a series of short light pulses separated by times long compared to the fluorescence decay times. A common mode of dynamic

fluorescence measurement is what is called the frequency domain [4,5,19,20,29,30]. In a frequency-domain measurement the excitation process is continuously repetitive at a rate that is comparable to the fluorescence decay rate. The fluorescence response to this continuous repetitive excitation wave train is measured, averaged, and analyzed over a time long compared to the longest relaxation time of the fluorescence. The signal of the fluorescence response is analyzed in terms of the frequency components (Fourier components) of the measured repetitive fluorescence signal. The modulation and phase of the separate frequency components of the fluorescence signal are compared to the frequency components of the excitation light, and the fluorescence lifetimes are extracted using frequency-domain analysis [4,7,19,20,31–37]. Both the frequency- and time-domain methods are complementary and theoretically equivalent, being related through Fourier transforms. We now define the nomenclature for the polar plot description.

Single Lifetime Measurements

The simplest frequency-domain measurement uses sinusoidally modulated excitation light. The fluorescence signal is modulated at the same frequency as the excitation. However, depending on the frequency of the excitation, the amplitude of the sinusoidal fluorescence signal will be demodulated (relative to the fractional demodulation of the excitation) and the phase of the fluorescence signal will lag that of the excitation light. The phase shift and demodulation of the fluorescence signal relative to the excitation signal gives information about the lifetime distribution of the fluorophores probed. For this simple case, the excitation light is of the form [7].

$$E(t) = E_0 + E_\omega \cos(\omega t + \varphi_E) \tag{3}$$

where ω is the frequency of the excitation modulation and E_0 and E_ω are the DC (long time average of the fluorescence signal) and AC (the amplitude of the oscillation component) of the excitation. The phase of the excitation light is known, and we denote it by φ_E. The depth of the modulation of the excitation light M_E is defined as E_ω/E_0. Every frequency component of the excitation wave train must produce a corresponding frequency component of the fluorescence. In the case of a pure sinusoidal excitation (Eq. (3)), the fluorescence signal can be expressed as:

$$S(t) = S_0 + S_\omega \cos(\omega t + \varphi_S), \tag{4}$$

which has a corresponding phase φ_S and depth of modulation, M_S. A usual frequency-domain experiment measures the relative phase shift $\varphi = \varphi_S - \varphi_E$ and the relative depth of modulation, $M = M_S/M_E$. For a single lifetime system, where all fluorophores have the same fluorescence lifetime, the relationship between that lifetime and the measured parameters is [4,20,30]:

$$\varphi(\tau) = \arctan(\omega\tau), \tag{5}$$

and

$$M(\tau) = \frac{1}{\sqrt{1 + (\omega\tau)^2}}. \tag{6}$$

The phase and modulation are two separate quantities of the fluorescence signal that are measured for any single frequency of the excitation. According to Eqs. (5) and (6), two separate lifetimes can be determined, one from the phase and one from the modulation. Only for a single lifetime system are these two lifetimes equal. For a multiple lifetime system, the apparent lifetimes calculated from Eqs. (5) and (6) will not be equal. A complete frequency-domain analysis, in the case of a complex system with more than one lifetime, requires that measurements of phase and modulation be carried out at several frequencies. Then it is possible to extract multiple fluorescence lifetimes and amplitudes from a fluorescence frequency dispersion curve (if information about one lifetime component is known, then the lifetime information of a second component and their ratio can be determined [31]). However, even in the case of a distribution of lifetimes, measurements of φ and M at a single frequency often suffice to provide the necessary information about a system.

Measurements of Multiple Lifetime Systems at a Single Frequency

We now introduce the parameters needed to define the polar plot representation. Consider a collection of multiple fluorescent species, which have a distribution of lifetimes. For any given ensemble of fluorophores, the total steady-state intensity from all fluorophores with the lifetime τ would be:

$$S_0(\tau) = \beta \sum_i c_i(\tau)\varepsilon_i(\tau)Q_i(\tau), \tag{7}$$

where the sum is over all fluorescent species. $c_i(\tau)$ is the concentration of species i with lifetime τ. Likewise, $\varepsilon_i(\tau)$ and $Q_i(\tau)$ are the absorption coefficient and the quantum yield of the ith species with a lifetime τ. β is an instrumentation constant such that the sum over all lifetime components, $\int_\tau S_0(\tau)\,d\tau$, is the total intensity of the signal. $S_0(\tau)$ is then the intensity distribution function for those species with lifetime τ.

For each different value of lifetime, τ, at any particular frequency there would be a phase and modulation (Eqs. (5) and (6)) corresponding to a fluorescence

response described in Eq. (4). The total signal is the intensity-weighted sum of the component signals. We can write the equivalent of Eq. (4) as:

$$\begin{aligned} S_{\text{tot}}(t) &= S_{0\,\text{tot}} + S_{\omega\,\text{tot}}\cos(\omega t + \varphi_{\text{tot}}) \\ &= \int_\tau (S_0(\tau) + S_\omega(\tau)\cos(\omega t + \varphi(\tau)))\,d\tau \\ &= \int_\tau (S_0(\tau))(1 + [S_\omega(\tau)/S_0(\tau)]\cos(\omega t + \varphi(\tau)))\,d\tau \\ &= \int_\tau (S_0(\tau))(1 + M(\tau)\cos(\omega t + \varphi(\tau)))\,d\tau \qquad (8) \end{aligned}$$

For distinct lifetime components $S_0(\tau)$ and $S_\omega(\tau)$ would be delta functions multiplied by the appropriate amplitude. If we divide the second term of Eq. (8) by $S_{0\,\text{tot}}$, we get Eq. (9) for the time varying part in terms of the signal modulation,

$$M_{\text{tot}}\cos(\omega t + \varphi_{\text{tot}}) = \int_\tau [S_0(\tau)/S_{0\,\text{tot}}]M(\tau) \times \cos(\omega t + \varphi(\tau))\,d\tau. \qquad (9)$$

Using a trigonometric identity, we write:

$$M_{\text{tot}}(\cos\varphi_{\text{tot}}\cos\omega t + \sin\varphi_{\text{tot}}\sin\omega t) = \int_\tau [S_0(\tau)/S_{0\,\text{tot}}]\, M(\tau)(\cos\varphi(\tau)\cos\omega t + \sin\varphi(\tau)\sin\omega t)\,d\tau. \qquad (9A)$$

We define $I(\tau) = [S_0(\tau)/S_{0\,\text{tot}}]$ where $I(\tau)$ is the fraction (or distribution function) of the steady-state intensity that is emitted from fluorophores with lifetime τ. The measured phase shift is not the average of the phase shifts, nor is the measured modulation the average of the modulations. The measured φ_{tot} and M_{tot} are weighted sums (integrals) of all the participating components. Equation (9A) splits into two parts giving Eqs. (10) and (11), where we drop the $\cos(\omega t)$ and $\sin(\omega t)$ terms common on both sides of the equations:

$$M_{\text{tot}}\cos\varphi_{\text{tot}} = \int_\tau I(\tau)M(\tau)\cos\varphi(\tau)\,d\tau, \qquad (10)$$

and

$$M_{\text{tot}}\sin\varphi_{\text{tot}} = \int_\tau I(\tau)M(\tau)\sin\varphi(\tau)\,d\tau. \qquad (11)$$

We can separate φ_{tot} and M_{tot} from Eqs. (10) and (11) to get separate equations for the total phase shift and total modulation, which are the only measured parameters:

$$\tan\varphi_{\text{tot}} = \frac{\int_\tau I(\tau)M(\tau)\sin\varphi(\tau)\,d\tau}{\int_\tau I(\tau)M(\tau)\cos\varphi(\tau)\,d\tau}, \qquad (12)$$

and

$$M_{\text{tot}}^2 = \left(\int_\tau I(\tau)M(\tau)\sin\varphi(\tau)\,d\tau\right)^2 + \left(\int_\tau I(\tau)M(\tau)\cos\varphi(\tau)\,d\tau\right)^2. \qquad (13)$$

The equivalent of these equations have been derived in many previous publications [7], and references therein. The lifetimes calculated from φ_{tot} and M_{tot} will in general not be equal. They are equal only in the case of a single lifetime. The extent to which the two lifetimes differ gives information about the distribution function, $I(\tau)$. Because M and φ are related for any given τ (that is, for any single value of τ, if we know φ we can calculate M, and vise versa), and because they are the only two parameters that are measured separately, we can only expect to measure two independent parameters defining the distribution function for each measurement of φ_{tot} and M_{tot}.

A CHANGE OF COORDINATES TO DERIVE THE POLAR PLOT

Because of the non-linearity of Eqs. (12) and (13), the relation between the measured phase and modulation and the actual lifetime distribution can be difficult to interpret. But, we can change variables into a coordinate system where the single lifetime components add directly to give the total measured signal [10,11,14,18,38].

Referring to Eqs. (10) and (11), we change coordinates to x and y according to the equations:

$$x = M(\tau)\cos\varphi(\tau) \qquad (14)$$

$$y = M(\tau)\sin\varphi(\tau). \qquad (15)$$

This is the decomposition of a vector of magnitude $M(\tau)$ onto the x- and y-axes in terms of the polar angular coordinate $\varphi(\tau)$. $\varphi(\tau)$ and $M(\tau)$ are the phase and modulation of each separate fluorescence component with lifetime τ. On this x–y plot, M is the distance from the origin and φ is the angle from the x-axis (see Fig. 1). This decomposition is equivalent to the description of the fluorescence dynamics in the complex plane where the y-axis is the imaginary axis and x is the real axis ([6], and the Appendix C). Referring to Eqs. (10) and (11), and Eqs. (14) and (15), we can write:

$$M_{\text{tot}}\cos\varphi_{\text{tot}} = x_{\text{tot}} = \int_\tau I(\tau)x(\tau)\,d\tau \qquad (16)$$

and

$$M_{\text{tot}}\sin\varphi_{\text{tot}} = y_{\text{tot}} = \int_\tau I(\tau)y(\tau)\,d\tau. \qquad (17)$$

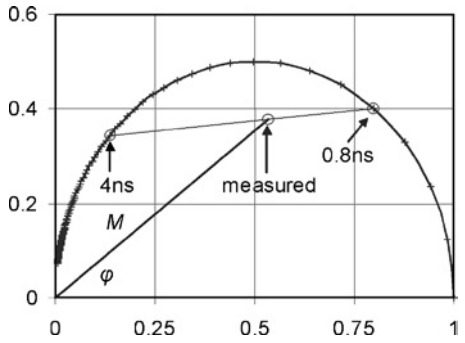

Fig. 1. A simulated plot of lifetime locations measured at 100 MHz. The semicircle is the single lifetime curve. The location {1,0} represents 0 lifetime. The location {0,0} represents infinite lifetime. Lifetimes increase counter-clockwise to the left. In this coordinate system the measured value is the intensity-weighted average of the two component lifetimes. All different ratios of the two lifetime components would fall on the line between them. For example, as shown, components with lifetimes of 4 and 0.8 ns (here the short lifetime has two-thirds the probability/intensity of the long lifetime), the measured lifetime is, phase: 1.1, and modulation: 1.8 ns.

We can construct a vector

$$\vec{r}_{\text{tot}} = \begin{bmatrix} x_{\text{tot}} \\ y_{\text{tot}} \end{bmatrix}, \text{ so that } \vec{r}_{\text{tot}} = \int_{\tau} I(\tau)\vec{r}(\tau)\,d\tau. \qquad (18)$$

$\vec{r}_{\text{tot}}$ is now the intensity-weighted average of the $\vec{r}(\tau)$ in the polar plot coordinate system (in the complex plane, the real and imaginary axes, see Appendix C). This is a convenient visualization of the measured phase and modulation and allows valuable information about the lifetime distribution function to be extracted and easily visualized. This is the decomposition used commonly in Cole–Cole plots of dielectric relaxation [38]. Clayton *et al*. [18] have discussed some properties of this representation for fluorescence data.

Fluorescence Signals with a Single Lifetime Component

Figure 1 shows a typical reference curve for single lifetimes plotted in this coordinate system. Different frequencies will give different values on this semicircle, but single lifetimes will always lie on the semicircle defined by the points {0, 0}, {1, 0}, and {0.5, 0.5} (see Appendices A and C for proofs of this statement). This is a universal curve for any single lifetime component. The points on the semicircle are the measured values of the vector $\vec{r}(\tau)$ *only* for single lifetimes.

Fluorescence Signals with more than One Lifetime Component

The location of the measured points for a general multi-lifetime measurement will be the intensity-weighted average of the contributions of the vectors of the separate components. For example, for two lifetimes (see Eq. (18)):

$$\vec{r}_{\text{tot}} = a\vec{r}_a + b\vec{r}_b. \qquad (19)$$

The location of $\vec{r}_{\text{tot}}$ is simply the relative intensity-weighted average of the location on the chord line between $\vec{r}_a$ and $\vec{r}_b$ (see Fig. 1 and Appendix C). The average of the two distinct single lifetime components, each of which lie separately on the single lifetime semicircle, would no longer be on the semicircle. Thus, a difference in modulation lifetime and phase lifetime is immediately apparent in this plot as a deviation from the semicircle, and indicates multiple lifetimes.

For any particular decaying system, measurements at a certain frequencies are more sensitive to a given lifetime range than other frequencies. For instance, on this plot it would be hard to resolve differences in lifetimes found in the region near the origin. In Appendix B we discuss how to find the most sensitive frequency region for particular underlying frequency components in this representation, and conditions that are best for identifying component contributions.

Because the location of any measurement is the weighted average of the locations of its constituent components, the locations of the components define vertices of a polygon in which the measurement must lie. For example, in the simplest case of a two-component system the location of the measurement will be on the line between the locations of the two components (Fig. 1 and Appendix C); a three-component system would define a triangle, and more components would define the vertices of a polygon. Because a single measurement can only determine two parameters, in practice, the case of three known components (a triangle) is the most complex case of interest (more than two parameters are needed to determine the ratios for any polygon of higher order than a triangle). However, if a part of the lifetime distribution is known, it can be reduced to a single vector, reducing the overall complexity of the analysis.

LIFETIME DISTRIBUTIONS

Often, an ensemble of a fluorescent species does not decay with a single lifetime. A frequency-domain lifetime measurement with such a sample would not lie on the semicircle. This is true for any fluorescence lifetime distribution, as described earlier. Therefore, if multiple fluorescent species are present, each emitting with more than one lifetime or a distribution of lifetimes, the points on the polar coordinate diagram corresponding to each separate

fluorescent species will not lie on the semicircle. However, the same analysis can be performed provided that the point on the polar coordinate diagram for each separate fluorescent species (which could have more than one lifetime, and does not lie on the semicircle polar plot) remains constant during the measurement; that is, if the shape of the lifetime distribution of each species does not change. This point can then be used in the analysis in the same manner as discussed earlier for separate, single lifetime components. The location of the lifetime distribution for a specific fluorophore in the polar coordinate system can be used as a lifetime-spectroscopic marker to identify that dye. This significantly reduces the importance of knowing the exact lifetime distribution of the fluorophores, emphasizing the contribution of the species to the signal. This also greatly reduces the parameters necessary for interpreting the data and considerably relaxes the requirement on error bounds in the measurement. The points of measurements are located on the polar plot without carrying out a fitting procedure to determine the time decay parameters of the separate components. The locations of the points on the polar plot are determined solely from fitting the phase and modulation of the fluorescence measurement without further analysis. The fluorescing species can be categorized in a FLIM image by their location on the polar plot (see Fig. 6 for an example). This does not replace the traditional full analysis of component lifetime analysis; but, especially for FLIM data, where lifetime distributions are routinely observed and signal-to-noise is relatively low, the polar plot analysis is very valuable to locate lifetime species, or lifetime distributions.

For example, a mixture of two dyes each of which has two lifetimes is a four lifetime component system, but can be treated as a two point system in the same manner as the two lifetime component system discussed earlier. Each of the dyes would have a set location defined by their two lifetimes. These locations are constant if the fractions of the two lifetime components remain the same when measuring mixtures with different ratios of fluorescent species; that is, in the case where only the intensity ratio between the two dyes is variable. Therefore, as in a two-component case, the measurement would lie on a straight line connecting the two points defined by the separate lifetime distribution of each of the two dyes, just as in the case for two single lifetime components. The only unknown parameter is the ratio between the two dyes. This means, in this case, the number of unknown parameters in the analysis is related to the number of fluorescent species, and not the total number of lifetimes in the distribution. One can therefore measure the phase and modulation of the constituent fluorescent species separately, and those locations can be used as constant points in the analysis of the mixture. We emphasize this because this illustrates that the description of the measurement is more general than may seem at first, and does not require single lifetime components. The data representation for the different chemical species with lifetime distributions can be treated and identified just as in the case of separate, single lifetime components.

PROBLEMS CAUSED BY ARTIFACTS: PHOTO-BLEACHING

True fluorescence measurements can only be located in the area below the single lifetime semicircle. Measured points lying above this semicircle curve represent physically invalid (impossible) lifetime distributions; however, actual data might fall outside the valid region of the polar plot due to other factors (noise, photo-bleaching, artifacts interfering with the measurement, etc.). Figure 2 is an example showing how the data can be affected by photo-bleaching. Photo-destruction of fluorophores can be a major problem during FLIM data acquisition. If not recognized, this can lead to false interpretations. However, once diagnosed, it is possible to take photo-bleaching into account in the analysis. If possible, data with photo-bleaching present should not be fit to a sine wave, but to

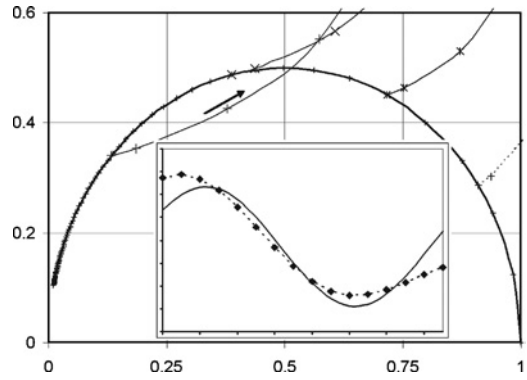

Fig. 2. Photo-bleaching effect. Shown are several lifetimes (4, 2, 1, and 0.5 ns at 100 MHz) and how the measurement deviates from the single lifetime curve with increasing dynamic photo-bleaching contribution to the measured signal. Locations that are outside of the semicircle are physically impossible through any combination of lifetimes, but measurements with photo-bleaching or other artifacts may cause the calculated points to lie outside of the semicircle. The initial direction taken by the curves with increasing rates of photo-bleaching is dependent on the instrument setup, especially on the actual order in time of the phase measurements (whether they are increasing, decreasing, or what the starting phase is). Large amounts of photo-bleaching will always result in large modulations from the fitting procedure, meaning that there will always be a general trend away from the origin. Inset is an example data showing the photo-bleached signal and the fit to a sine.

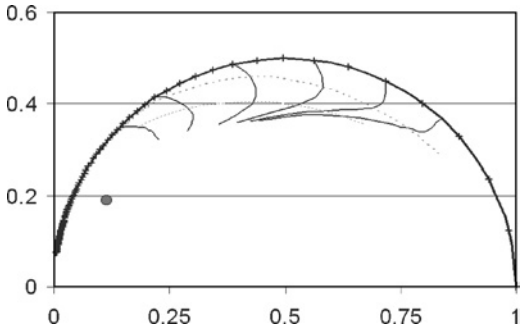

Fig. 3. Gaussian lifetime distributions. Plotted with solid lines are the locations for the measurement of Gaussian distributions with varying width and fixed peak lifetimes. In dashed lines are the trends for varying peaks with fixed width. Because negative lifetimes are cutoff (physically impossible), increasing the width of the Gaussian moves the trend towards the location marked with a dot (if negative lifetimes were permitted, the trends would move more towards the center of the semicircle). The dot represents the location if all lifetimes are equally present. One can see that the effect of the negative cutoff is more pronounced for short lifetimes. In practice, only relatively small widths would be observed in Gaussian distributions, or the distributions would be more like that in Eq. (20). Note that the trends are non-intersecting, meaning that a single measurement can find the peak and width of any Gaussian distribution.

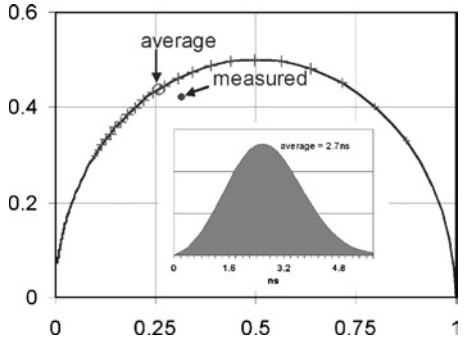

Fig. 4. Broad lifetime distribution: In the insert is shown a lifetime distribution of the form of Eq. (22) with average lifetime of 2.7 ns. Highlighted in the main chart are those single lifetimes with a considerable contribution to the average. The measured location is the weighted average of the single lifetime locations (phase: 2.14, modulation: 2.57 ns).

a sine wave multiplied by the appropriate decay function of photo-bleaching to remove the effect of the photo-bleaching. If a measured point lies above the semicircle on this plot, this is diagnostic of such an artifact, Fig. 2.

EXAMPLES

Gaussian Lifetime Distributions

Figure 3 shows how the locations of a Gaussian distribution in the polar plot change with changing peak and width. Except in the case of extremely wide distributions the locations are close to, but not on the semicircle.

For a more realistic case, consider a continuous lifetime distribution with an intensity distribution of the form,

$$I(\tau) = \frac{N\tau}{\sqrt{\sigma}} e^{-(\tau-\tau_c)^2/\sigma} \quad \text{for} \quad 0 < \tau \leq \tau_0, \qquad (20)$$

where N is a normalization constant. The intensity of a fluorophore with a single natural radiative lifetime of τ_0 is proportional to τ/τ_0, where τ is the measured lifetime of the fluorophore (this could be, for instance, the case for conditions where $\tau < \tau_0$ because dynamic quenching or energy transfer is present—or any process changing the lifetime). $I(\tau)$ is a partial Gaussian lifetime distribution with the weighting factor, τ. $I(\tau)$ is zero at $\tau = 0$ ($\tau < 0$ is undefined and physically impossible) and $\tau > \tau_0$ is not possible. Only two parameters, σ and τ_c, define the shape of the distribution (assuming τ_0 is known). The location of the measured $\vec{r}(\tau)$ is the weighted average of all of the single lifetime locations, Eq. (18). A typical location of the measured $\vec{r}(\tau)$ is close to the single lifetime location for the peak lifetime τ_c (which is on the semicircle) but shifted towards the center of the semicircle (location $\{0.5, 0\}$ on the polar plot). The location of the measured point is shifted clockwise along the standard semicircle curve due to the unequal spacing of the lifetime points as one progresses along the semicircle (see Fig. 4). A single lifetime measurement would be sufficient to determine the two parameters (the peak and the width) of the distribution represented by Eq. (20), as discussed earlier. This location is now characteristic of the distribution and forms an equivalent single vector that can be combined with other vectors (that also belong to distributions) as earlier.

Fluorescein and KI Equilibrium Mixture: Single Lifetime

Figure 5 shows data taken from a series of measurements of an equilibrium solution of fluorescein mixed with different concentrations of iodide at a pH of 9. Iodide quenches the fluorescein resulting in lower fluorescence intensities and shorter lifetimes. The fluorescence decays with a single lifetime at every concentration of the iodide, and the lifetime is dependent on the concentration of the iodide. Figure 5 shows the results of experiments demonstrating how the lifetime of the fluorescein follows the semicircle as the concentration of iodide increases.

Fluorescein and KI with Fast Mixing: Multiple Lifetimes

Figure 6 shows fluorescein mixed with iodide in a microsecond fast mixer [9,39,40]. The turbulent mixing

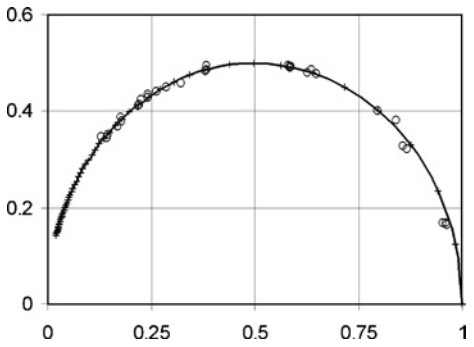

Fig. 5. Fluorescein (100 μM) and different concentrations of the dynamic quencher, iodide (KI), are mixed to shorten the single lifetime. As the concentration of iodide changes, the values of the lifetimes move along the single lifetime semicircle, indicating a single lifetime system.

creates regions of unmixed and completely mixed fluorescein that change their relative volumes as the mixing progresses. The mixer is a continuous flow design where the solutions, after initial contact in the mixing chamber, flow in a jet stream (moving at 100 m/s). The mixing is complete in microseconds, and the distance along the stream where the mixing progresses is imaged onto a full-field fluorescence lifetime-resolved imaging instrument. The data is taken in points along the mixing channel, so each point represents progressive times as the mixing proceeds. The lifetimes are determined at every pixel of the image along the flow pattern. In this case, there is more than one lifetime, and the data lies below the semicircle. However, the data points nearly follow a straight line between the two end points (on the semicircle), which shows

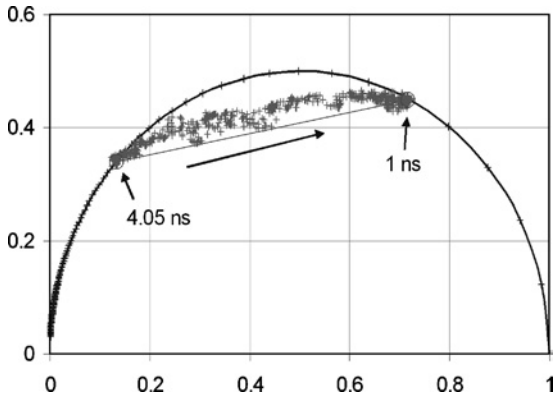

Fig. 6. Fluorescein (10 μM) and iodide (500 mM) are mixed using a fast turbulent mixer (see text). The lifetime distribution is dominated by a two lifetime system, with the relative probabilities of the unmixed and fully mixed lifetimes changing with time. Here time course of the mixing experiment is increasing from the long lifetime (left side) to the short lifetime (right side). The total mixing time is $\sim$15 μs.

that the fluorescence signal is dominated by two lifetime components. There is a noticeable slight curvature to the data, deviating from a straight line, which is due to other lifetimes appearing in the distribution [8,40]. This shows the great advantage of plotting the data of all points of the image (the phase and modulation are measured at every pixel of the image). The interpretation in terms of the fluorescing species and their stochiometric ratio, follows directly from the polar plot, without a detailed analysis to separate and fit the components in the usual way.

CONCLUSION

In very rapid measurements of lifetimes in images (with 10^4–10^6 pixels) it is often not possible to carry out the measurement on the full image with more than one frequency of modulation. Therefore, one misses the opportunity available in cuvette (single channel) measurements where extensive averaging leads to high signal-to-noise and multi-frequency data can be acquired. We have demonstrated that useful, quantitative, diagnostic information can be attained quickly and efficiently from single-frequency measurements using the polar plot analysis. Reliable information about the fractional contribution to the fluorescence signal from separate lifetime distributions (for instance a Gaussian system or even more complex lifetime distributions) can be extracted in a relatively straightforward and time-efficient manner, similar to what can also be achieved with multiple single lifetime components. If only two single lifetime species are present, the result must lie on the straight line chord on the polar plot between the locations of the single lifetime components. The position of the data point on the straight line tells us the relative fraction of each lifetime component. The savings in measurement/analysis time and the visual acuity of the analysis and plot are especially valuable for image analysis of frequency-domain FLIM data. Artifacts such as photolysis can also often easily be identified. The phase and modulation parameters of the lifetime measurements can be analyzed using known specific models to give more information about the lifetime distributions, especially by tuning the parameters of the fluorophores by changing the solution conditions (e.g. quenching, FRET, polarity, ion concentrations, interacting ligands), and by changing the ratios of the different fluorescing species (Fig. 6). Much useful diagnostic qualitative and quantitative information can be extracted by simply observing the distribution of the measured points in the polar plots of Figs. 1–6, and this information is available in real time. We have also noted analogies of the polar plot of frequency-domain data to commonly used analytical techniques in the field of dielectric relaxation, as well as chemical relaxation

kinetics and simple circuit analysis (Appendix C). Although the basic underlying theory describing all these relaxation techniques is the same, there has been little overlap in the methods of analysis. The analysis methods presented here, and also discussed by [18], have proved to be exceptionally useful in dielectric relaxation for decades. We anticipate that this will also to be of value for the analysis of fluorescence lifetime-resolved imaging data, in particular for image diagnostics.

APPENDIX A: SEMICIRCLE

To show that single lifetimes form a semicircle, invert the equations (Eqs. (3) and (4)) relating the phase and modulation to the lifetime to get:

$$\omega\tau = \tan\varphi \tag{A.1}$$

and

$$\omega\tau = \sqrt{1/M^2 - 1} \tag{A.2}$$

We set these equal to each other. In our coordinate system this is

$$y/x = \sqrt{1/(x^2 + y^2) - 1}. \tag{A.3}$$

This is simplified to give

$$x^2 + y^2 = x, \tag{A.4}$$

which defines a semicircle with radius 0.5 and centered at $\{0.5, 0\}$ in the first quadrant.

APPENDIX B: OPTIMUM FREQUENCY

For any given lifetime there is an optimum frequency which the system should be run at to give the best resolution at that lifetime. From Eqs. (12) and (13) we get

$$\frac{\partial M}{\partial \tau} = \frac{\tau\omega^2}{(1 + \tau^2\omega^2)^{3/2}} \tag{B.1}$$

and

$$\frac{\partial \varphi}{\partial \tau} = \frac{\omega}{1 + \tau^2\omega^2}. \tag{B.2}$$

For a single lifetime we can construct a radius of change from these two equations and optimize it for ω.

$$R^2 = \left(\frac{\tau\omega^2}{(1 + \tau^2\omega^2)^{3/2}}\right)^2 + \left(\frac{\omega}{1 + \tau^2\omega^2}\right)^2. \tag{B.3}$$

$$\frac{\partial R^2}{\partial \omega} = 0 = \left(\frac{4\tau^2\omega^3}{(1 + \tau^2\omega^2)^3} - \frac{6\tau^4\omega^5}{(1 + \tau^2\omega^2)^4}\right) + \left(\frac{2\omega}{(1 + \tau^2\omega^2)^2} - \frac{4\tau^2\omega^3}{(1 + \tau^2\omega^2)^3}\right) \tag{B.4}$$

$$\frac{\partial R^2}{\partial \omega} = 0 = \frac{2\omega + 4\tau^2\omega^3 - 4\tau^4\omega^5}{(1 + \tau^2\omega^2)^4} \tag{B.5}$$

$$\omega_{\text{best}^2} = \frac{1 + \sqrt{3}}{+2\tau^2}. \tag{B.6}$$

For example, measurements near 4 ns should be made at 47 MHz; measurements near 1 ns should be made at 186 MHz. A 100 MHz system would be optimal for measurements at 1.9 ns.

APPENDIX C: POLAR PLOT REPRESENTATION IN THE COMPLEX PLANE

The derivation of the formalism of this paper in terms of vectors in the complex plane, and the analogy to dielectric dispersion, is now given.

In many areas in physics the description of frequency-domain experiments is given in terms of phasors, and usually the essentials are presented in beginning physics classes. This appendix is a short account of the formalism in the complex plane, which is the usual formalism used in dielectric relaxation and chemical kinetics. The basic idea as applied to fluorescence is very simple, and involves writing the fundamental equations in terms of complex numbers. The fluorescence response to excitation light is written as convolution integral in Eq. (2), where the fluorescence response to a very short pulse of light is given in Eq. (1). The excitation light (driving function) is either a sinusoidal repetition (Eq. (3)) or a sum of sinusoidal components (a Fourier expansion). If we assume a single sinusoidal excitation function, then by writing the sinusoidal excitation as $E(t) = E_0/2[e^{-j\omega t} + e^{j\omega t}]$, we can derive the fluorescence response of a single fluorescence decay component [6] (the response to a delta pulse of light is $F(t) = F_0 e^{-t/\tau}$) as $F(t) = E_0 F_0 \tau + \frac{E_\omega F_0 \tau}{1 + j\omega\tau} e^{j[\phi_c + \omega t]}$; $j = \sqrt{-1}$. The last exponential term represents simply the complex representation of the time-dependent sinusoidal oscillation of the fluorescence signal. Many separate fluorescence components with different lifetimes will simply contribute linearly as separate components of a summation,

$$F(t) = E_0\left[\sum\nolimits_i F_{0,i}\tau_i\right] + E_\omega\left[\sum\nolimits_i \frac{F_{0,i}\tau_i}{1 + j\omega\tau_i}\right] e^{j[\phi_c + \omega t]}.$$

By subtracting the constant (steady-state fluorescence) term, dividing by $E_0F_0 = E_0\Sigma_i F_{0,i}\tau_i$, and dropping the oscillating sinusoidal dependence (it is the amplitude of this exponential that we detect with synchronous methods) we then have $P(\tau) = \frac{E_\omega}{E_0F_0}[\Sigma_i \frac{F_{0,i}\tau_i}{1 + j\omega\tau_i}] =$

$\frac{E_\omega}{E_0}[\Sigma_i \frac{F_{0,i}\tau_i}{F_0}\frac{1}{1+j\omega\tau_i}] = \frac{E_\omega}{E_0}[\Sigma_i \alpha_i \frac{1}{1+j\omega\tau_i}]$, where $\Sigma_i\alpha_i = 1$. $P(\tau)$ is the frequency-dependent amplitude. This equation is now in a form that we can easily analyze by inspection. The term $[\Sigma_i \alpha_i \frac{1}{1+j\omega\tau_i}]$ has the same form as the usual description of dielectric relaxation experiments of multiple independent relaxing components, and this valuable formalism has been used since 1928 [38,41]. All separate relaxing components can be plotted in the complex plane with the same complex function, $1/(1 + j\omega\tau)$ (all components fall on the same semicircular plot—see later).

We have given this polar plot description in terms of vectors in the complex plane in order to show the compatibility of the description of frequency-domain fluorescence with the dielectric relaxation and chemical kinetic relaxation literature. Specifically, the general type of analysis we present in Fig. 1, the semicircle track for a single relaxing component and similar diagrams [14], is widely known in the field of dielectric relaxation as the Cole–Cole plot [38]. There is a very large literature, including text books, on the subject [10,11,14,15]. Here we examine some useful properties that are easily derived from the polar plot of $1/(1 + j\omega\tau)$ in the complex plane formalism. The discussion is somewhat different than that in the original publications, but the formalism is the same. $z = \Sigma_i \alpha_i \frac{1}{1+j\omega\tau_i}$ is a complex number that can be written as

$$\sum_i \alpha_i \frac{1 - j\omega\tau_i}{1 + \omega^2\tau_i^2} = \sum_i \alpha_i \left[\frac{1}{1 + \omega^2\tau_i^2} - \frac{j\omega\tau_i}{1 + \omega^2\tau_i^2}\right]$$
$$= \sum_i \alpha_i z_i = \sum_i \alpha_i \,[\mathrm{Re}z_i + j\mathrm{Im}z_i],$$

in terms of its real and imaginary parts, and this can be plotted as a vector in the complex plane. The lengths of the separate vectors (z_i for each separate fluorescence component) are $|z_i| = \frac{1}{\sqrt{1+\omega^2\tau_i^2}}$, which means they each have a maximum possible length of one (when $\omega = 0$), and a minimum of zero (when $\omega = \infty$). As the frequency increases, each vector z_i will rotate counterclockwise with an angle of $\theta_i = \tan^{-1}(\omega\tau_i)$; in other words, each vector can be written as $z_i = \frac{1}{\sqrt{1+\omega^2\tau_i^2}} e^{j\theta_i}$.

It is especially easy in this formalism to show that each vector (in the complex plane) separately traverses a semicircular path, as shown in Fig. 1 and Appendix A. One forms a new vector, $z_i' = z_i - 1/2$. In other words, the complex number z_i is the sum of the real number 1/2 plus a new complex vector z_i', so that $z_i = z_i' + 1/2$. The magnitude of the z_i' vector is easily shown to be $|z_i'| = (z_i' * z_i')^{1/2} = 1/2$. Since the magnitude is independent of $\omega\tau_i$, the path traversed by each Z_i vector is on a circle of radius 1/2.

In an early publication dealing with microwave absorption in liquids [17] (see also page 296 of Hill *et al.* [11]), an analysis was presented demonstrating that two separate relaxation times will appear on a Cole–Cole plot along the chord on the semicircle connecting the two points that correspond to the two separate relaxation phenomena (see Fig. 1). This is identical to the formalism presented in our paper, and in the paper by Clayton *et al.* [18]. It is very easy to derive this result using the formalism of this appendix. Each of the separate relaxations is represented, as shown earlier, by a separate vector (in the complex plane) on the normalized semicircle; $\vec{A} = 1/(1 + j\omega\tau_A)$ and $\vec{B} = 1/(1 + j\omega\tau_B)$. The contribution of each separate process to the measured signal $\vec{C}$ is represented by $\vec{C} = \alpha\vec{A} + \beta\vec{B}$, where $\alpha + \beta = 1$. We define a vector $\vec{D}$, such that $\vec{A} + \vec{D} = \vec{B}$ ($\vec{D}$ is the chord between $\vec{A}$ and $\vec{B}$). By simple substitution, $\vec{C} = \vec{A} + \beta\vec{D} = \vec{B} - \alpha\vec{D}$. Thus, the point represented by $\vec{C}$ lies on $\vec{D}$; that it, $\vec{C}$ must lie along the straight line between the points $\vec{A}$ and $\vec{B}$. The position of the measured point $\vec{C}$ on the chord $\vec{D}$ is just $\beta\vec{D}$ from $\vec{A}$ and $-\alpha\vec{D}$ from $\vec{B}$. This is indicated in Fig. 1; α and β are the weighting factors defining the distances from each vector apex. The distance along the cord has the same relationship to the weighting of the components as the lever law of mechanics. We refer the reader to the vast literature of dielectric relaxation given earlier for further discussion, and for numerous applications using similar formalisms and diagrams.

REFERENCES

1. D. V. O'Conner and D. Phillips (1984). *Time-correlated Single Photon Counting*, Academic Press, London.
2. D. W. Piston, G. Marriott, T. Radivoyevich, R. M. Clegg, T. M. Jovin, and E. Gratton (1989). Wide-band acousto-optic light modulator for frequency domain fluorometry and phosphorimetry. *Rev. Sci. Instrum.* **60**, 2596–600.
3. B. Valeur (2002). *Molecular Fluorescence Principles and Applications*, Wiley VCH, New York.
4. R. D. Spencer and G. Weber (1969). Measurements of subnanosecond fluorescence lifetime with a cross-correlation phase fluorometer. *Ann. Acad. Sci.* **158**, 361–76.
5. E. Gratton, D. M. Jameson, and R. Hall (1984). Multifrequency phase and modulation fluorometry. *Ann. Rev. Biophys. Bioeng.* **13**, 105–124.
6. R. M. Clegg and P. C. Schneider (1996). Fluorescence Lifetime-resolved Imaging Microscopy: a general description of the lifetime-resolved imaging measurements. in J. Slavik (Ed.), *Fluorescence Microscopy and Fluorescent Probes*, Plenum Press, New York, pp. 15–33.
7. G. Redford and R. M. Clegg (2005). Chapter 11: Real-time fluorescence lifetime imaging and FRET using fast gated image intensifiers. In A. Periasamy and R. N. Day (Ed.), *Molecular Imaging: FRET Microscopy*, American Physiological Society Methods in Physiology Series, Oxford University Press, Oxford, pp. 193–226.

8. G. Redford (2003). Rapid lifetime imaging. In *Biophysical Society Meeting* (Vol 84, No. 2), San Antonio, TX.
9. Z. Majumdar, J. D. B. Sutin, and R. M. Clegg (2003), Microsecond kinetics in a continuous flow turbulent mixer- detection with fluorescence intensity and fluorescence lifetime imaging. In *34th Annual Meeting of the Biophysical Society*. *Biophys. J.* **84**(2).
10. C. J. F. Bottcher and P. Bordewijk (1978). Theory of electric polarization. In *Dielectrics in Time-Dependent Fields*, 2nd ed., Vol. II, Elsevier, New York.
11. N. E. Hill *et al*. (1969). *Dielectric Properties and Molecular Behavior*, van Nostrand Reinhold Company, New York, p. 480.
12. J. L. Ribeiro and L. G. Vieira (2003). The factorized form for dielectric relaxation. *Eur. Phys. J. B* **36**, 21–26.
13. Y.-Z. Wei and S. Sridhar (1993). A new graphical representation for dielectric data. *J. Chem. Phys.* **99**(4), 3119–3124.
14. A. K. Jonscher (1983). *Dielectric Relaxation in Solids*, Chelsea Dielectrics Press, London.
15. G. G. Raju (2003). Dielectrics in electric fields. in H. L. Willis (Ed.), *Power Engineering*, Marcel Dekker, New York, p. 578.
16. F. H. Mueller (Ed.) (1953). Das Relaxationsverhalten der Materie: 2. Marburger Diskussionstagung. In *Sonderausgabe der Kolloid-Zeitschrift*, Vol. 134, Darmstadt, Dr. Dietrich Steinkopft, p. 224.
17. K. Bergmann, D. M. Roberti, and C. P. Smyth (1960). Analysis in terms of two relaxation times for some aromatic ethers. *Microwave Absorption and Molecular Structure in Liquids*, Vol. XXXI, p. 665.
18. A. H. A. Clayton, Q. S. Hanley, and P. J. Verveer (2004). Graphical representation and multicomponent analysis of single-frequency fluorescence lifetime imaging microscopy data. *J. Microsc.* **213**(1), 1–5.
19. D. M. Jameson, E. Gratton, and R. D. Hall (1984). The measurement and analysis of heterogeneous emissions by multifrequency phase and modulation fluorometry. *Appl. Spectrosc. Rev.* **20**(1), 55–106.
20. J. B. Birks and I. H. Munro (1967). *Prog. React. Kinet.* **4,** 239.
21. R. S. Becker (1969). *Theory and Interpretation of Fluorescence and Phosphorescence*, Wiley Interscience, New York, p. 283.
22. T. Förster (1951). *Fluoreszenz Organischer Verbindungen*, Göttingen, Vandenhoeck & Ruprecht, p. 315.
23. J. R. Lakowicz (1999). *Principles of Fluorescence Spectroscopy*, 2nd ed., Kluwer Academic/Plenum, New York.
24. D. J. S. Birch and R. E. Imhof (1991). Time-domain fluorescence spectroscopy using time-correlated single-photon counting. in J. Lackowicz (Ed.), *Topics in Fluorescence Spectroscopy*, Plenum Press, New York, pp. 1–88.
25. M. J. Cole *et al*. (20001). Time-domain whole-field fluorescence lifetime imaging with optical sectioning. *J. Microsc.* **203**(3), 246–257.
26. K. Dowling *et al*. (1999). High resolution time-domain fluorescence lifetime imaging for biomedical applications. *J. Modern Optics* **46**(2), 199–209.
27. P. F. Gottling (1923). The determination of the time between excitation and emission for certain fluorescent solids. *Phys. Rev.* **22**, 566–573.
28. R. B. Cundall and R. E. Dale (Eds.) (1983). *Time-resolved fluorescence spectroscopy in biochemistry and biology*. in F. Nato (Ed.), *NATO ASI Series. Series A, Life Sciences*, Vol. 69, Advanced Study Institute on Time-Resolved Fluorescence Spectroscopy in Biochemistry and Biology, Saint Andrews, 1980, Plenum Press, New York, p. 785.
29. F. Dushinsky (1993). *Z. Phys.* **81**, 7–21.
30. J. B. Birks and D. J. Dawson (1961). *J. Sci. Instrum.* **38**, 262.
31. T. W. J. Gadella, T. M. Jovin, and R. M. Clegg (1993). Fluorescence lifetime imaging microscopy (FLIM)-Spatial resolution of microstructures on the nanosecond time scale. *Bioimaging* **2**, 139–59.
32. T. W. J. J. Gadella, R. M. Clegg, and T. M. Jovin (2001). Fluorescence lifetime imaging microscopy: Pixel-by-pixel analysis of phase-modulation data. *Bioimaging* **2**(3), 139–59.
33. M. J. Booth and T. Wilson (2004). Low-cost, frequency-domain, fluorescence lifetime confocal microscopy. *J. Microsc.* **214**(1), 36–42.
34. O. Holub *et al*. (2000). Fluorescence lifetime-resolved imaging (FLI) in real-time—A new technique in photosynthetic research. *Photosynthetica* **38**(4), 581–599.
35. V. Squire and Bastiaens (2000). Multiple frequency fluorescence lifetime imaging microscopy. *J. Microsc.* **197**(2), 136–149.
36. R. M. Clegg, O. Holub, and C. Gohlke (2003). Fluorescence lifetime-resolved imaging: Measuring lifetimes in an image. *Meth. Enzymol.* **360**, 509–542.
37. P. I. H. Bastiaens and A. Squire (1999). Fluorescence lifetime imaging microscopy: Spatial resolution of biochemical processes in the cell. *Trends Cell Biol.* **9**(2), 48–52.
38. K. S. Cole and R. H. Cole (1941). Dispersion and absorption in dielectrics. *J. Chem. Phys.* **9**, 341.
39. Z. Majumdar, J. D. B. Sutin, and R. M. Clegg (2005). A microfabricated continuous-flow turbulent mixer for the study of fast reaction kinetics, manuscript in press, Review of Scientific Instruments.
40. G. I. Redford, Z. K. Majumdar, J. D. B. Sutin, and R. M. Clegg (2005). Properties of microfluidic turbulent mixing, revealed by fluorescence lifetime imaging, manuscript in press, Journal of Chemical Physics.
41. K. S. Cole (1928). Electrical impedence of suspensions of spheres. *J. Gen. Physiol.* **12**, 29–54.